

## Antilocalization and spin-orbit coupling in the hole gas in strained GaAs/In<sub>x</sub>Ga<sub>1-x</sub>As/GaAs quantum well heterostructures

G. M. Minkov and A. A. Sherstobitov

*Institute of Metal Physics RAS, 620219 Ekaterinburg, Russia*

A. V. Germanenko, O. E. Rut, and V. A. Larionova

*Institute of Physics and Applied Mathematics, Ural State University, 620083 Ekaterinburg, Russia*

B. N. Zvonkov

*Physical-Technical Research Institute, University of Nizhni Novgorod, 603600 Nizhni Novgorod, Russia*

(Received 28 September 2004; published 15 April 2005)

Anomalous low-field magnetoresistance in *p*-type strained quantum wells is studied. It is experimentally shown that the Bychkov-Rashba mechanism leads to the cubic in quasimomentum spin-orbit splitting of the hole energy spectrum and the antilocalization behavior of low-field magnetoresistance is well described by the Hikami-Larkin-Nagaoka expression.

DOI: 10.1103/PhysRevB.71.165312

PACS number(s): 73.20.Fz, 73.61.Ey

The combination of quantum coherence and spin rotation produces a number of interesting transport properties. Numerous proposals for electronic devices that use spin-orbit coupling have appeared in the last few years, including gate-controlled sources and detectors of spin-polarized current.<sup>1-3</sup> Spin-orbit coupling results in the spin splitting of the energy spectrum when an inversion symmetry is lifted. The lack of inversion symmetry of the original crystal results in the splitting of the energy spectrum, which is linear and cubic in in-plane quasi-momentum,  $k$ . This splitting is described by terms known as the Dresselhaus terms.<sup>4</sup> In low-dimensional systems an additional mechanism of spin splitting is caused by the asymmetry of the confining potential (so called the Bychkov-Rashba term<sup>5</sup>). In two-dimensional (2D) semiconductor systems this asymmetry arises from asymmetry of the smooth electrostatic potential in the perpendicular to the 2D plane direction, from Schottky barrier potential, from asymmetry in doping layer dispositions, and the composition gradient along the growth direction. It is very important that this asymmetry can be controlled by gate voltage. For electron 2D states, the Bychkov-Rashba term is linear in  $k$ . For 2D hole systems, the situation becomes more complicated because of fourfold degeneracy of the topmost valence band  $\Gamma_8$  of the parent material. Theoretical considerations of this problem and experimental studies show that the splitting is cubic in  $k$  in this case.<sup>6-9</sup>

The measurements of interference-induced low-field magnetoresistance are the powerful tool for studies of the spin-splitting, spin-, and phase-relaxation mechanisms. At present, there are numerous studies of *n*-type 2D systems,<sup>2,10-16</sup> whereas the more complicated *p*-type systems are studied noticeably less<sup>17-21</sup> (for more references see the review article by Zawadzki and Pfeffer<sup>22</sup>). As for the strained quantum well, the antilocalization and spin relaxation in the 2D hole gas are practically not investigated in these systems.

In this paper, we present the results of an experimental study of the low-field magnetoresistance caused by weak antilocalization in *p*-type strained GaAs/In<sub>x</sub>Ga<sub>1-x</sub>As/GaAs

quantum well structures. It has been found that the magnetoresistance shape is well described by the Hikami-Larkin-Nagaoka (HLN) expression,<sup>23</sup> which means that the leading term in the spectrum splitting is cubic in quasimomentum. We show that in contrast to *n*-type systems, where such a finding implies that the Dresselhaus spin-splitting mechanism is the main, the Bychkov-Rashba mechanism is responsible for the spin splitting of the hole energy spectrum in the strained quantum wells under investigation.

The GaAs/In<sub>x</sub>Ga<sub>1-x</sub>As/GaAs heterostructures were grown by metal-organic vapor phase epitaxy on semi-insulator GaAs substrate. The quantum well was biaxially compressed due to the lattice mismatch between In<sub>x</sub>Ga<sub>1-x</sub>As and GaAs. Two types of heterostructures were studied. The structures of the first type, 3855, 3856, and 3857, consist of a 250 nm thick undoped GaAs buffer layer, a carbon  $\delta$ -layer, a 7 nm spacer of undoped GaAs, an 8 nm In<sub>0.2</sub>Ga<sub>0.8</sub>As well, a 7 nm spacer of undoped GaAs, a carbon  $\delta$ -layer, and 200 nm cap layer of undoped GaAs (see Fig. 1). The structure of the second type, 3951, was analogous, the only difference was the wider spacer, 15 nm, and hence the higher mobility. The structures within the first group differ by carbon density in  $\delta$ -layers. The parameters of the structures are presented in Table I. The samples were mesa etched into standard Hall bars and then an Al gate electrode was deposited by thermal evaporation onto the cap layer through a mask. Varying the gate voltage  $V_g$  from  $-1$  to  $+3$  V, we changed the hole density in the quantum well from  $1 \times 10^{12}$  to  $3 \times 10^{11}$  cm<sup>-2</sup>. The analysis of the temperature dependence of the Shubnikov-de Haas oscillations showed that the hole effective mass was equal to  $(0.160 \pm 0.005)m_0$  and did not depend on the hole density.

Figure 2 shows the low-field magnetoconductivity,  $\Delta\sigma(B) = \rho_{xx}^{-1}(B) - \rho_{xx}^{-1}(0)$ , measured at  $T = 0.44$  K for structure 3857 as a function of a normalized magnetic field  $b = B/B_{tr}$ , where  $B_{tr} = \hbar/(2el^2)$  with  $l$  as the mean free path. The antilocalization maximum at  $B = 0$  in the conductivity-versus-magnetic field curves decreases with lowering hole density

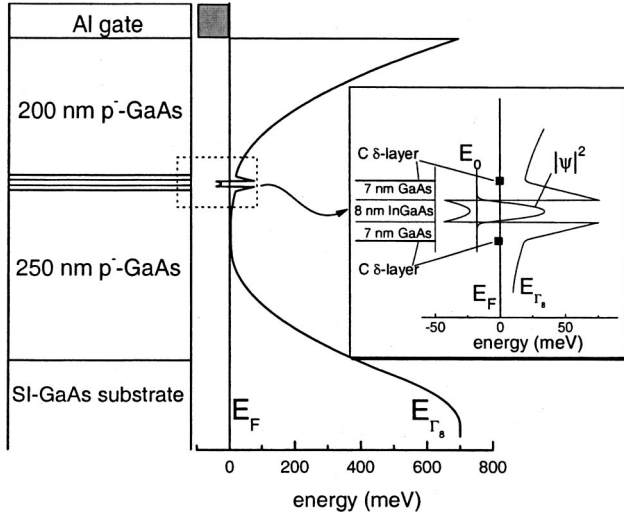


FIG. 1. The cross section of structure 3857 and its energy diagram.

and disappears at  $V_g = 2.75$  V, when  $p \approx 3.8 \times 10^{11} \text{ cm}^{-2}$ . In the structure 3951 with the higher hole mobility, the disappearance happens at  $p \approx 3 \times 10^{11} \text{ cm}^{-2}$ .

Theoretically, the low-field anomalous magnetoresistance was studied in Refs. 11, 23, and 25. It was shown that when the spin splitting is cubic in  $k$ , the magnetoconductivity curve should be described by the Hikami-Larkin-Nagaoka (HLN) expression

$$\begin{aligned} \frac{\Delta\sigma(b)}{G_0} = & \psi \left[ \frac{1}{2} + \frac{\tau_1}{b} \left( \frac{1}{\tau_\phi} + \frac{1}{\tau_s} \right) \right] - \ln \left[ \frac{\tau_1}{b} \left( \frac{1}{\tau_\phi} + \frac{1}{\tau_s} \right) \right] \\ & + \frac{1}{2} \psi \left[ \frac{1}{2} + \frac{\tau_1}{b} \left( \frac{1}{\tau_\phi} + \frac{2}{\tau_s} \right) \right] - \frac{1}{2} \ln \left[ \frac{\tau_1}{b} \left( \frac{1}{\tau_\phi} + \frac{2}{\tau_s} \right) \right] \\ & - \frac{1}{2} \psi \left( \frac{1}{2} + \frac{\tau_1}{b} \frac{1}{\tau_\phi} \right) + \frac{1}{2} \ln \left( \frac{\tau_1}{b} \frac{1}{\tau_\phi} \right). \end{aligned} \quad (1)$$

Here,  $G_0 = e^2 / (2\pi^2 \hbar)$ ,  $\tau_\phi$  and  $\tau_s$  are the phase and spin relaxation times, respectively,  $\psi(x)$  is the digamma function, and  $\tau_n$ ,  $n=1$ , is the transport relaxation time,

$$\frac{1}{\tau_n} = \int W(\theta) (1 - \cos n\theta) d\theta, \quad (2)$$

where  $W(\theta)$  stands for the probability of the scattering by an angle  $\theta$ .

TABLE I. The parameters of structures investigated.

Structure	$N_1$ ( $\text{cm}^{-2}$ ) <sup>a</sup>	$N_2$ ( $\text{cm}^{-2}$ ) <sup>a</sup>	$p$ ( $\text{cm}^{-2}$ )	$\mu$ [ $\text{cm}^2$ (V s) <sup>-1</sup> ]
3855	$4 \times 10^{11}$	$3 \times 10^{11}$	$4.7 \times 10^{11}$	4800
3856	$8 \times 10^{11}$	$6 \times 10^{11}$	$7.5 \times 10^{11}$	5700
3857	$1.2 \times 10^{12}$	$8 \times 10^{11}$	$9.5 \times 10^{11}$	8000
3951	$1.2 \times 10^{12}$	$8 \times 10^{11}$	$5.4 \times 10^{11}$	13100

<sup>a</sup> $N_1$  and  $N_2$  are the carbon density in outer and inner  $\delta$ -layers, respectively.

For the Dyakonov-Perel spin-relaxation mechanism,<sup>24</sup> which is dominant at low temperatures, the value of  $\tau_s$  is determined by the spin-orbit splitting of the energy spectrum,  $\hbar\Omega_3 \propto k^3$ , as

$$\frac{1}{\tau_s} = 2\Omega_3^2 \tau_3, \quad (3)$$

where  $\tau_3$  is defined by Eq. (2).

Taking into account both the cubic and linear terms leads to more complicated expression (see Ref. 25). The following two parameters describing the spin relaxation arise in this case

$$\frac{1}{\tau'_s} = 2\Omega_1^2 \tau_1 \quad (4)$$

and

$$\frac{1}{\tau_s} = 2(\Omega_1^2 \tau_1 + \Omega_3^2 \tau_3), \quad (5)$$

where  $\hbar\Omega_1$  is the linear in  $k$ ,  $\hbar\Omega_1 \propto k$ , spin-orbit splitting.

Comparison of the experimental data with theoretical expressions for two limiting cases, when only the cubic or linear term is taken into account, is shown in Fig. 3. To span the characteristic minima in  $\Delta\sigma$ -versus- $B$  curves, the fitting interval has been chosen as  $-0.3B_{tr} < B < 0.3B_{tr}$ . Strictly speaking, the boundaries of this interval do not satisfy the diffusion approximation  $B \ll B_{tr}$  in which framework the formulas<sup>23,25</sup> for magnetoconductance have been derived. Nevertheless, one can see that taking into account only the linear term does not allow us to describe satisfactorily the magnetoconductivity shape within the fitting interval while the HLN expression gives a good agreement. Beyond the diffusion regime, the HLN theory was generalized by Zdun-

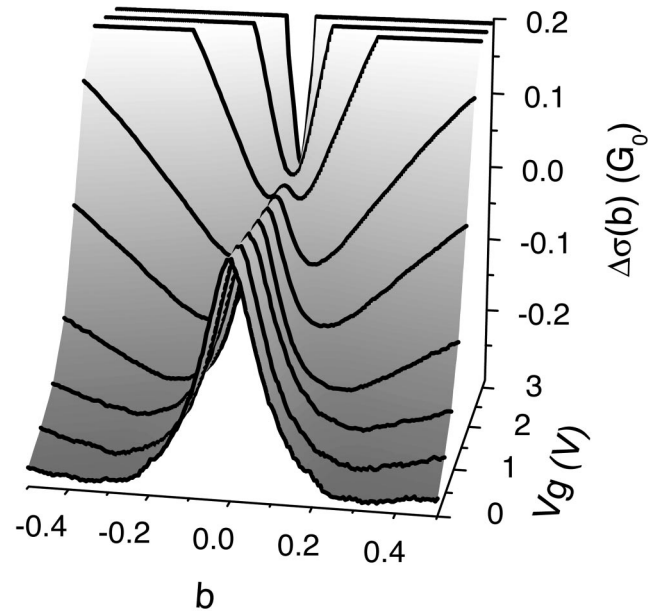


FIG. 2. The magnetoconductivity plotted against the reduced magnetic field for different gate voltages, structure 3857, and  $T = 0.44$  K.

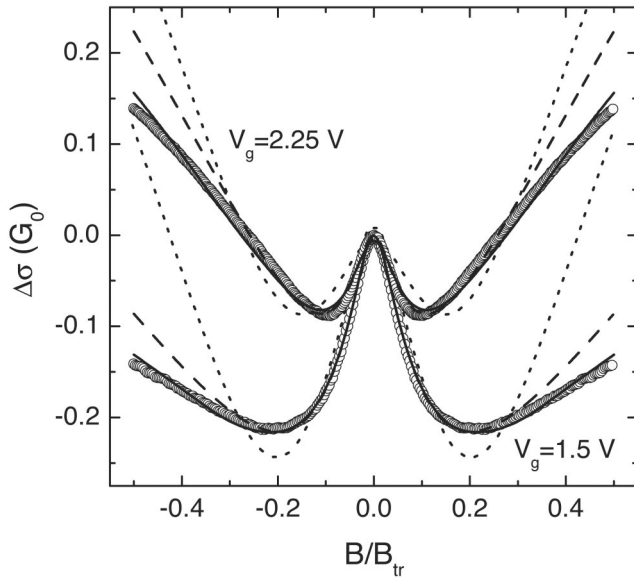


FIG. 3. The magnetoconductivity as a function of the normalized magnetic field measured on the structure 3857 at  $T=0.44$  K for the two gate voltages:  $V_g=1.5$  V ( $p=8 \times 10^{11}$  cm $^{-2}$ ,  $\tau_1=5.4 \times 10^{-13}$  s) and  $V_g=2.25$  V ( $p=5.8 \times 10^{11}$  cm $^{-2}$ ,  $\tau_1=3.9 \times 10^{-13}$  s). Symbols are the experimental data. The dotted lines are the best fit by Eq. (13) from Ref. 25 when the only linear in  $k$  term is taken into account. Dashed lines are the best fit by the HLN expression, Eq. (1). Solid lines are the results of the simulation procedure (see the Appendix) which is valid beyond the diffusion approximation. The fit has been done within the magnetic field range  $-0.3B_{tr} < B < 0.3B_{tr}$ . The fitting parameters are given in Table II.

iaik *et al.*<sup>13</sup> However, the final expressions are very complicated and inconvenient to use in the fitting procedure. Because of this, we used the simulation approach described in our paper, Ref. 26. To take into account the spin-relaxation processes, Eq. (20) from this paper was modified as described in the Appendix. As Fig. 3 illustrates, with the use of Eq. (A1) we obtain a nice coincidence of calculated and measured curves over the whole magnetic field range. Although the theory beyond the diffusion approximation describes the magnetoresistance curve better, the fitting parameters  $\tau_1/\tau_\phi$  and  $\tau_1/\tau_s$  are found to be close to those obtained with the help of Eq. (1) (see Table II). Therefore, it seems natural to analyze the experimental results with the use of the more simple HLN expression.

Further indication that just the cubic in  $k$  splitting is responsible for the spin relaxation is reasonable behavior of the fitting parameters obtained from Eq. (1) with the temperature change. As seen from Fig. 4 the parameter  $\tau_\phi$  exhibits the behavior close to  $T^{-1}$ -law that corresponds to the phase relaxation caused by inelasticity of electron-electron interaction.<sup>27</sup> The parameter  $\tau_s$  is temperature independent as should be for degenerated electron gas. Such analysis has been carried out for all the structures investigated and the results are collected in Fig. 5 as a plot of the spin relaxation time  $\tau_s$  against the hole density controlled by the gate voltage.

For the first sight the fact that the magnetoconductance curves are well described by the HLN expression means that

TABLE II. The parameters of the best fit for the data presented in Fig. 3 as obtained taking into account only the linear in  $k$  term (Ref. 25), only the cubic in  $k$  term in the diffusion approximation (Ref. 23), and the cubic in  $k$  term beyond the diffusion approximation (see the Appendix).

$V_g$ (V)	Theory	$\tau_1/\tau_\phi$	$\tau_1/\tau_s$
1.5	Ref. 25	0.020	0.178
	Ref. 23	0.016	0.051
	Appendix	0.014	0.040
2.25	Ref. 25	0.034	0.142
	Ref. 23	0.017	0.032
	Appendix	0.013	0.025

the Dresselhaus cubic term gives the main contribution to the spin splitting in the structure investigated. Whether or not it is so, one can understand analyzing the hole density dependence of spin-orbital splitting,  $\hbar\Omega_3(p)$ . For the Dresselhaus mechanism, the splitting should be proportional to  $p^{3/2}$  because  $\Omega_3 = \gamma k^3/4$ , where  $\gamma$  is the constant depending only on the band parameters of the parent material (see Appendix A in Ref. 11 for details). Experimentally, the value of spin-orbit splitting  $\hbar\Omega_3$  can be found from Eq. (3) using  $\tau_s$  obtained above and  $\tau_3$ . How the quantity  $\tau_3$  has been obtained is considered below.

As seen from Eq. (2) the relaxation time  $\tau_3$  is determined by the scattering anisotropy via the function  $W(\theta)$ . Just the same function determines the relationship between the quantum and transport relaxation times,  $\tau_0$  and  $\tau_1$ , respectively. Therefore, we estimate  $\tau_3$  using the experimental value for  $\tau_0$ ,

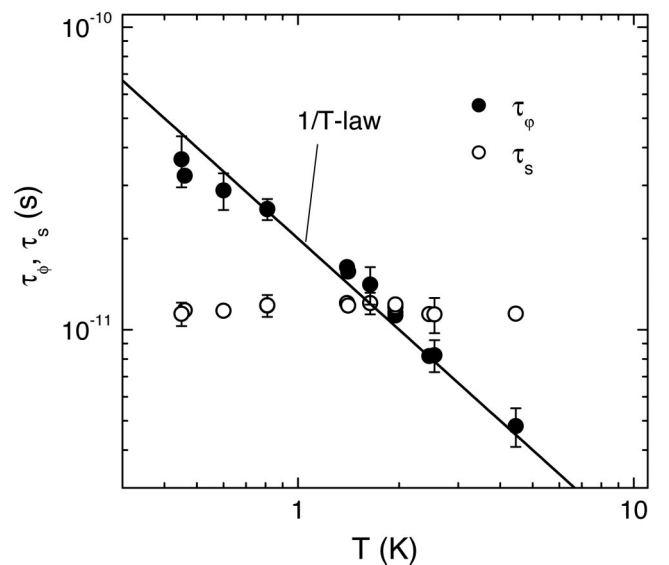


FIG. 4. The temperature dependence of the phase and spin relaxation time as obtained from the fit of the experimental data by Eq. (1) for structure 3857 at  $V_g=1.5$  V. Solid line is the  $T^{-1}$ -law.

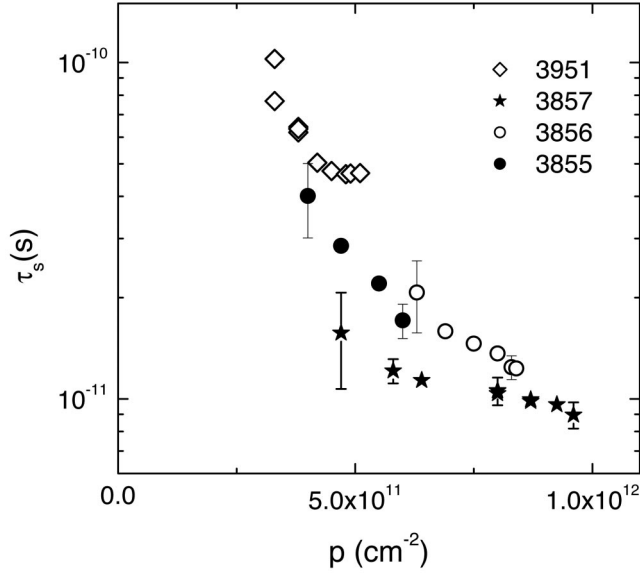


FIG. 5. The spin relaxation time as a function of hole density controlled by the gate voltage for all structures investigated,  $T = 0.44$  K.

$$\tau_3 = \tau_0 \int W(\theta) d\theta / \int W(\theta) (1 - \cos 3\theta) d\theta, \quad (6)$$

and conceiving the physically reasonable angle dependence for  $W(\theta)$  so that the ratio

$$K_{01} = \int W(\theta) (1 - \cos \theta) d\theta / \int W(\theta) d\theta \quad (7)$$

is equal to the experimental quantity  $\tau_0/\tau_1$ . The value of  $\tau_0$  has been obtained from the analysis of the magnetic field dependence of the amplitude of the Shubnikov–de Haas oscillations, while  $\tau_1$  has been found from the mobility value,  $\tau_1 = \mu m/e$ . The experimental hole density dependences of  $\tau_0$  and  $\tau_1$ , presented in Fig. 6, show that the scattering is really anisotropic in all the structures and the  $\tau_0$  to  $\tau_1$  ratio lies in the interval from 0.2 to 0.5. This seemingly points to the fact that the scattering is mainly determined by ionized impurities and  $W(\theta)$  can be chosen in the form obtained, e.g., in Ref. 29. However, our estimation shows that the electron mobility in this case should be one to two orders of magnitude higher than that observed experimentally. We suppose that the roughness of the quantum well interfaces restricts the mobility in our structures. This mechanism is theoretically studied in Ref. 30, where the explicit form for  $W(\theta)$  is derived and it is shown that the scattering anisotropy strongly depends on the parameter  $\Lambda$  characterizing the fluctuations of the quantum well width due to interfaces roughness. Using the form for  $W(\theta)$  from this paper we have chosen such a value of parameter  $\Lambda$  which satisfies the equality between the experimental value of  $\tau_0/\tau_1$  and the calculated from Eq. (7) value of  $K_{01}$ . Then, with this  $\Lambda$  value we have calculated the  $\tau_3$ -to- $\tau_0$  ratio. Doing so we have found that  $\tau_3 = (0.7, \dots, 0.8)\tau_0$  when  $K_{01}$  lies within actual for our case range,  $K_{01} = 0.2, \dots, 0.5$ . Note, the close results,  $\tau_3 \approx \tau_0$ , are obtained if

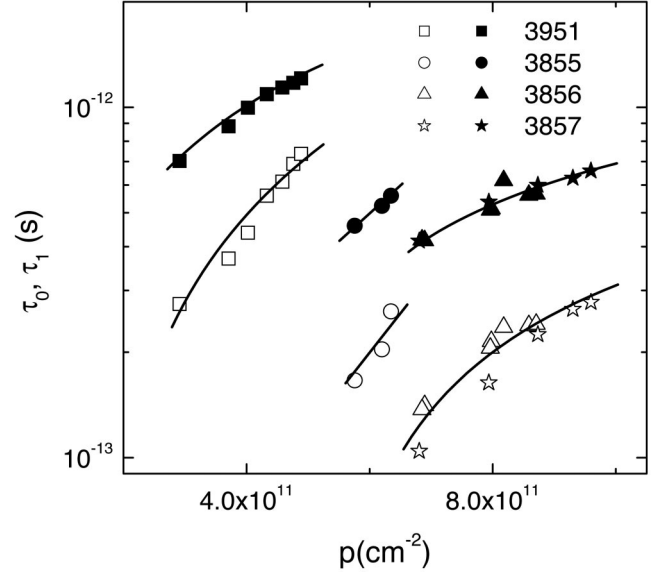


FIG. 6. The hole density dependence of  $\tau_0$  (open symbols) and  $\tau_1$  (solid symbols). Solid lines are provided as a guide for the eye.

one uses  $W(\theta)$  corresponding to scattering by remote ionized impurities.<sup>29</sup>

Finally, we arrive at the key figure of the paper, Fig. 7, where the value of spin splitting  $\hbar\Omega_3 = \hbar/\sqrt{2}\tau_3\tau_s$  is plotted as a function of the hole density. One can see that (i) we do not observe the characteristic for the cubic in  $k$  spin-orbit splitting  $p^{3/2}$  dependence of  $\hbar\Omega_3$  and (ii) the different structures have significantly different values of the splitting for a given hole density. Both these facts unambiguously show that the

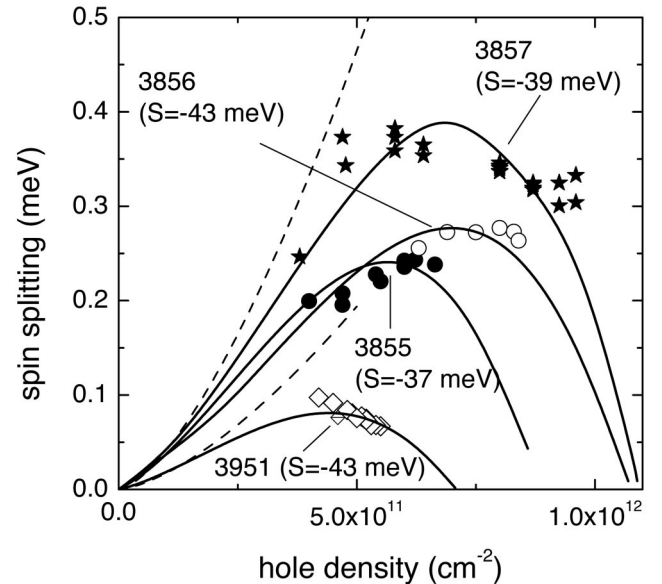


FIG. 7. The hole density dependence of the spin-orbit splitting for different samples. Symbols are the experimental data obtained as  $\hbar\Omega_3 = \hbar/\sqrt{2}\tau_3\tau_s$ , solid lines are calculation results (see text), and dashed lines show  $p^{3/2}$ -law for structures 3856 and 3951. In brackets, the values of the fitting parameter  $S$  for each structure are shown.

Dresselhaus mechanism is not responsible for the cubic in  $k$  spin-orbit splitting of the hole spectrum.

Let us now discuss specific features of the Bychkov-Rashba effect for holes in strained quantum well heterostructures. In general, this effect in hole 2D systems is considered in Refs. 6–9. It has been qualitatively shown that the states of the heavy in  $z$ -direction holes forming the ground 2D subband do not have the linear in  $k$  term in spin-orbit splitting. This phenomenon can be understood as follows.<sup>31</sup> Terms of first order in the wave vector components can couple only those states which differ in projection of the angular momentum by one. The heavy hole states in a [001] QW have the angular momentum projection to the growth axis equal to  $\pm 3/2$ . Therefore the spin-orbit Hamiltonian mixing these states should contain third degrees of the wave vector components (in the axial approximation). This situation is opposite to the electronic case where two spin states  $\pm 1/2$  differ in spin projection by one, allowing for  $k$ -linear spin splitting.

Below we write out only the main expressions which help us to describe the experimental results quantitatively. We restrict our consideration by the case when only three hole bands are taken into account. They are the heavy- and light-hole  $\Gamma_8$  bands and the  $\Gamma_7$  hole band split off by spin-orbit interaction. In this case, the energy spectrum is described by the  $6 \times 6$  Luttinger-Kohn Hamiltonian<sup>32</sup> which includes the terms responsible for the strain.<sup>33</sup> As shown in Ref. 34, the  $6 \times 6$  Hamiltonian can be decoupled into two independent  $3 \times 3$  matrices of the form

$$H = \begin{pmatrix} A_+ & C \mp iB & \sqrt{2} \pm iB/\sqrt{2} \\ C \pm iB & A_- & F \mp i\sqrt{3}/2B \\ \sqrt{2} \mp iB/\sqrt{2} & F \pm i\sqrt{3}/2B & D \end{pmatrix} \quad (8)$$

where

$$A_{\pm} = -(\gamma_1 \mp 2\gamma_2)k_z^2 - (\gamma_1 \pm \gamma_2)k^2 + E_{\Gamma_8}(z) + V(z) \pm S,$$

$$B = 2\sqrt{3}\gamma_3kk_z,$$

$$C = \sqrt{3}k^2(\gamma_2^2 \cos^2 2\theta + \gamma_3^2 \sin^2 2\theta)^{1/2},$$

$$D = -\gamma_1(k_x^2 + k_y^2) + E_{\Gamma_7}(z) + V(z),$$

$$F = 2\gamma_2(\sqrt{2}k_z^2 - k^2/\sqrt{2}).$$

Here,  $\gamma_i$  stand for  $\hbar^2 \gamma_i^J / (2m_0)$ , where  $\gamma_i^J$  are the Luttinger parameters,  $k_z$  is the wave vector along the [001] growth direction,  $k^2 = k_x^2 + k_y^2$ ,  $\theta$  is the angle between the in-plane wave vector and the [100] direction,  $V(z)$  is the macroscopic electric potential in the heterostructure,  $E_{\Gamma_8}$  and  $E_{\Gamma_7}$  are the energies of edges of corresponding bands, and

$$S = b \left( \frac{\sigma + 1}{\sigma - 1} \right) \frac{\Delta a}{a} \quad (9)$$

is the splitting of the  $\Gamma_8$  band due to strain caused by the lattice mismatch between GaAs and  $\text{In}_x\text{Ga}_{1-x}\text{As}$ . In Eq. (9),  $b$  stands for the axial deformation potential of the valence

band,  $\sigma$  is the Poisson's ratio,  $\Delta a$  is the lattice mismatch between materials of the quantum well and barrier, and  $a$  is the lattice constant of the quantum well material. Let us estimate characteristic energies for the case of GaAs/ $\text{In}_{0.2}\text{Ga}_{0.8}\text{As}$  heterostructure. The value of  $\Delta a/a$  is about 1.4%,  $\sigma$  is approximately equal to 1/3, and  $b$  is about  $-1.7$  eV so that the value of strain-induced splitting  $2|S|$  is approximately equal to 90 meV. This value is five to ten times greater than the Fermi energy in our case. We find the Bychkov-Rashba splitting of the hole energy spectrum using the ratio  $E_F/(2S)$  as a small parameter. The band parameters  $\gamma_i$  and  $\Delta = E_{\Gamma_7} - E_{\Gamma_8}$  are supposed independent of the  $z$  coordinate. Then, in isotropic approximation,  $\gamma_2 = \gamma_3 = \gamma$ , the energy spectrum of the upper split off band for our case can be written as follows:

$$E^{\pm} \simeq E \pm \hbar\Omega_3 \quad (10)$$

with

$$\hbar\Omega_3 = 6\gamma^2 k^3 \int dz |\psi|^2 \frac{d}{dz} \left( \frac{1}{E - E_{\Gamma_8}(z) - S - V(z)} - \frac{1}{E - E_{\Gamma_8}(z) - \Delta - V(z)} \right), \quad (11)$$

where  $\psi$  and  $E$  are solutions of the Schrödinger equation

$$A_+ \psi = E \psi. \quad (12)$$

It is clearly seen from Eq. (11) that the Bychkov-Rashba splitting for all 2D subbands formed from the upper hole band is cubic in  $k$  in contrast to the electron energy spectrum where it is linear in  $k$ .

Now we are in position to compare the experimental  $\hbar\Omega_3$ -vs- $p$  dependences with those calculated from Eqs. (11) and (12). To find the electric potential  $V(z)$ , the Schrödinger equation has been self-consistently solved with the Poisson equation. We have used the band parameters for  $\text{In}_{0.2}\text{Ga}_{0.8}\text{As}$ , which are obtained by the linear interpolation from the values of GaAs and InAs:  $\gamma_1^J = -9.5$ ,  $\gamma_2^J = -3.5$ ,  $\Delta = 0.35$  eV (the signs of the Luttinger parameters correspond to the increasing of energy into the valence band), and  $\delta E_v = E_{\Gamma_8}(\text{GaAs}) - E_{\Gamma_8}(\text{In}_{0.2}\text{Ga}_{0.8}\text{As}) = 75$  meV. As an example, the energy profile and the wave function for structure 3857,  $V_g = 0$ , is shown in Fig. 1. To describe the experimental  $\Omega_3$ -vs- $p$  dependence for each structure, the parameter  $S$  has been used as a fitting one. One can see from Fig. 7 that we are able to describe well the experimental results obtained for different samples in our model varying the  $S$ -value from one to the other structure only slightly. The different value of strain-induced splitting for different samples seems to be natural. It can result, for instance, from deviation of In-content from its nominal value. As for the value of the strain-induced splitting,  $2|S| \simeq 75-90$  meV, it corresponds to the lattice mismatch and In-content laying within the intervals 1.2–1.4% and 17–20%, respectively. Let us direct attention to the interesting detail. The  $\hbar\Omega_3$ -vs- $p$  dependence exhibits behavior corresponding to Eq. (11),  $\hbar\Omega_3 \propto p^{3/2}$ , only at low hole density,  $p < 2 \times 10^{11} \text{ cm}^{-2}$ . At higher hole density this dependence has a maximum and sign change (not shown in figure).

This feature is caused by the fact that the hole density is varied by means of variation of the gate voltage. Applying the gate voltage, we change not only the value of the Fermi quasimomentum but the energy profile of the quantum well as well. In this case the integral in Eq. (11) is not constant any more and gives additional  $p$  dependence in  $\Omega_3$ . Vanishing of spin-orbit splitting at some hole density means that the quantum well in this point becomes effectively symmetric. We realize that the approximations of large strain-induced splitting and  $z$  independence of  $\gamma_i$  parameters made above are crude enough. Moreover, the well boundaries can be smooth and different, and the In-content can vary across the quantum well. These factors being taken into account could, in principle, change the value of  $S$  obtained from the fit. However, this should not change our interpretation in the large case.

In summary, we have shown that the Bychkov-Rashba mechanism results in the cubic in  $k$  spin-orbit splitting of the hole energy spectrum in strained heterostructures. The magnetoresistance curve in this case is well described by the HLN expression, which allows us to find the spin splitting as a function of the hole density. We have found that this dependence is nonmonotonic at relatively high hole density due to the sensitivity of the quantum well profile to the gate voltage.

The authors are grateful to L. E. Golub for interesting discussions and valuable comments. This work was supported in part by the RFBR (Grant Nos. 01-02-16441, 03-02-16150, and 04-02-16626), the CRDF (Grant Nos. EK-005-X1 and Y1-P-05-11), the INTAS (Grant No. 1B290) and the Russian Program *Physics of Solid State Nanostructures*.

#### APPENDIX: NUMERICAL SIMULATION OF ANTILOCALIZATION

The weak localization phenomenon for a spinless particle using the numerical simulation of a particle motion over the

plane with randomly distributed scatterers is studied both within and beyond diffusion regime in Ref. 26. It has been shown that obtaining from the simulation procedure the parameters of closed paths, one can calculate the quantum interference correction to the conductivity and its magnetic field dependence [see Eq. (20) in the paper cited]. Taking into account the spin relaxation processes leads to the following expression for the interference quantum correction (this generalization will be considered in more detail elsewhere):<sup>28</sup>

$$\delta\sigma(b) = -\frac{2\pi G_0}{I_s d} \sum_i \cos(bS_i) \exp(-l_i \gamma_\phi) \times \left( -\frac{1}{2} + \exp(-l_i \gamma_s) + \frac{1}{2} \exp(-2l_i \gamma_s) \right), \quad (\text{A1})$$

where  $I_s$  is the total number of paths;  $d$  is the diameter of the area from which the particle starts to walk and in which it returns;  $l_i$  and  $S_i$  are the length and algebraic area of the  $i$ th closed path;  $\gamma_\phi$  and  $\gamma_s$  are the phenomenological parameters describing the phase and spin relaxation and corresponding in real systems to ratios  $\tau_1/\tau_\phi$  and  $\tau_1/\tau_s$ , respectively; the lengths and areas in this expression are measured in units of mean free path and squared mean free path, respectively; and summation runs over all closed paths. In order to treat the experimental results presented in this paper, we have first collected the parameters of closed paths  $l_i$  and  $S_i$  simulating the motion of particle as described in Ref. 26, and, then, we have used Eq. (A1) to fit the experimental curves with  $\gamma_\phi$  and  $\gamma_s$  as the fitting parameters.

- 
- <sup>1</sup>Y. Ohno, D. K. Young, B. Beschoten, F. Matsukura, H. Ohno, and D. D. Awschalom, *Nature (London)* **402**, 790 (1999).  
<sup>2</sup>X. F. Wang, P. Vasilopoulos, and F. M. Peeters, *Phys. Rev. B* **65**, 165217 (2002).  
<sup>3</sup>T. Koga, J. Nitta, H. Takayanagi, and S. Datta, *Phys. Rev. Lett.* **88**, 126601 (2002).  
<sup>4</sup>G. Dresselhaus, *Phys. Rev.* **100**, 580 (1955).  
<sup>5</sup>Y. A. Bychkov and E. I. Rashba, *J. Phys. C* **17**, 6039 (1984).  
<sup>6</sup>L. G. Gerchikov and A. V. Subashiev, *Fiz. Tekh. Poluprovodn. (S.-Peterburg)* **26**, 131 (1992) [*Sov. Phys. Semicond.* **26**, 73 (1992)].  
<sup>7</sup>R. Winkler, *Phys. Rev. B* **62**, 4245 (2000).  
<sup>8</sup>R. Winkler, H. Noh, E. Tutuc, and M. Shayegan, *Physica E (Amsterdam)* **12**, 428 (2002).  
<sup>9</sup>W. Xu and L. B. Lin, *J. Phys.: Condens. Matter* **16**, 1777 (2004).  
<sup>10</sup>G. L. Chen, J. Han, T. T. Huang, S. Datta, and D. B. Janes, *Phys. Rev. B* **47**, 4084 (1993).  
<sup>11</sup>W. Knap, C. Skierbiszewski, A. Zduniak, E. Litwin-Staszewska, D. Bertho, F. Kobbi, J. L. Robert, G. E. Pikus, F. G. Pikus, S. V. Iordanskii, V. Mosser, K. Zekentes, and Yu. B. Lyanda-Geller, *Phys. Rev. B* **53**, 3912 (1996).  
<sup>12</sup>W. Knap, A. Zduniak, L. H. Dmowski, S. Contreras, and M. I. Dyakonov, *Phys. Status Solidi B* **198**, 267 (1996).  
<sup>13</sup>A. Zduniak, M. I. Dyakonov, and W. Knap, *Phys. Rev. B* **56**, 1996 (1997).  
<sup>14</sup>T. Hassenkam, S. Pedersen, K. Baklanov, A. Kristensen, C. B. Sorensen, P. E. Lindelof, F. G. Pikus, and G. E. Pikus, *Phys. Rev. B* **55**, 9298 (1997).  
<sup>15</sup>J. B. Miller, D. M. Zumbuhl, C. M. Marcus, Y. B. Lyanda-Geller, D. Goldhaber-Gordon, K. Campman, and A. C. Gossard, *Phys. Rev. Lett.* **90**, 076807 (2003).  
<sup>16</sup>S. A. Studenikin, P. T. Coleridge, N. Ahmed, P. Poole, and A. Sachrajda, *Phys. Rev. B* **68**, 035317 (2003).  
<sup>17</sup>Ch. Schierholz, R. Kursten, G. Meier, T. Matsuyama, and U. Merkt, *Phys. Status Solidi B* **233**, 436 (2002).  
<sup>18</sup>S. J. Papadakis, E. P. De Poortere, H. C. Manoharan, J. B. Yau, M. Shayegan, and S. A. Lyon, *Phys. Rev. B* **65**, 245312 (2002).  
<sup>19</sup>S. Pedersen, C. B. Sorensen, A. Kristensen, P. E. Lindelof, L. E.

- Golub, and N. S. Averkiev, Phys. Rev. B **60**, 4880 (1999).
- <sup>20</sup>L. E. Golub and S. Pedersen, Phys. Rev. B **65**, 245311 (2002).
- <sup>21</sup>Y. Y. Proskuryakov, A. K. Savchenko, S. S. Safonov, M. Pepper, M. Y. Simmons, and D. A. Ritchie, Phys. Rev. Lett. **89**, 076406 (2002).
- <sup>22</sup>W. Zawadzki and P. Pfeffer, Semicond. Sci. Technol. **19**, R1 (2004).
- <sup>23</sup>S. Hikami, A. Larkin, and Y. Nagaoka, Prog. Theor. Phys. **63**, 707 (1980).
- <sup>24</sup>M. I. Dyakonov and V. I. Perel, Zh. Eksp. Teor. Fiz. **60**, 1954 (1971) [Sov. Phys. JETP **33**, 1053 (1971)].
- <sup>25</sup>S. V. Iordanskii, Yu. B. Lyanda-Geller, and G. E. Pikus, Pis'ma Zh. Eksp. Teor. Fiz. **60**, 199 (1994) [JETP Lett. **60**, 206 (1994)].
- <sup>26</sup>G. M. Minkov, A. V. Germanenko, V. A. Larionova, S. A. Negashev, and I. V. Gornyi, Phys. Rev. B **61**, 13 164 (2000).
- <sup>27</sup>B. L. Altshuler, A. G. Aronov, and D. E. Khmel'nitsky, J. Phys. C **15**, 7367 (1982).
- <sup>28</sup>I. V. Gornyi, private communication.
- <sup>29</sup>J. Lee, H. N. Spector, and V. K. Arora, J. Appl. Phys. **54**, 6995 (1983).
- <sup>30</sup>D. Zanato, S. Gokden, N. Balkan, B. K. Ridley, and W. J. Schaff, Semicond. Sci. Technol. **19**, 427 (2004).
- <sup>31</sup>R. Winkler, *Spin-orbit Coupling Effects in Two-dimensional Electron and Hole Systems*, Springer Tracts in Modern Physics Vol. 191 (Springer, Berlin, 2003).
- <sup>32</sup>J. M. Luttinger and W. Kohn, Phys. Rev. **97**, 869 (1955); J. M. Luttinger, *ibid.* **102**, 1030 (1956).
- <sup>33</sup>G. E. Bir and G. L. Pikus, *Symmetry and Strain Induced Effects in Semiconductors* (Wiley, Chichester, 1974).
- <sup>34</sup>D. A. Broido and L. J. Sham, Phys. Rev. B **31**, 888 (1985).